Microchim Acta (2016) 183:573–580
DOI 10.1007/s00604-015-1678-2

ORIGINAL PAPER

A resistive type humidity sensor based on crystalline tin oxide nanoparticles encapsulated in polyaniline matrix

Saroj K. Shukla[1] · **Sudheesh K. Shukla**[2] · **Penny P. Govender**[2] · **Eric S. Agorku**[2]

Received: 5 July 2015 / Accepted: 9 November 2015 / Published online: 13 November 2015

Abstract We have synthesized a nanocomposite consisting of crystalline tin oxide (SnO_2) nanoparticles and polyaniline (PANI) by in-situ *polymerization and composite formation* (IPCF). The structure and morphology was characterized using X-ray diffraction (XRD), Fourier transform infrared spectroscopy (FTIR) and transmission electron microscopy (TEM). The nanocomposite is shown to represent a viable material for electrical resistivity based sensing of humidity in the 5 to 90 % relative humidity (RH) range. The electrical resistance of the composite linearly decreases from 127.5 to 11.5 kΩ with humidity from 5 to 95 %. The sensitivity is 0.22 % RH^{-1}, the response time is 26 s, and the recovery time is 30 s. The fabrication of SnO_2/PANI composite combines the high sensitivity of SnO_2 towards moisture with good electrical conductivity of PANI, which influences the electronic properties of the material and enables the design of more efficient humidity sensors. The water vapor layering growth kinetics on the composite was investigated by isothermal thermogravimetric analysis and an interaction with limited diffusion aggregate type kinetics has been proposed.

Keywords Polyaniline-tin oxide nanocomposite · IPCF · Humidity sensor · Relative humidity

Introduction

The demand of sensitive, selective and reproducible humidity sensors have significantly increased due to their application in food processes and storage, environmental condition monitoring, agriculture, pharmaceutical and structural health monitoring [1, 2]. Nanostructured metal oxides are ideal materials for the fabrication of humidity sensors because of the ability to tailor their surface and charge-transport properties [3]. The intensively used metal oxides in humidity sensing are MgO, ZnO, and TiO_2 [4–6]. The oxide based humidity sensor suffers from undesired cross-sensitivity effects, low sensing range, and slow degree of out gassing and poor mechanical flexibility [7]. Among the different strategies to trim these draw backs, a combination of nanostructured metal oxide and conducting polymers such as polythiophene, polypyrrole, PEDOT and polyaniline (PANI) have been reported due to their synergistic effect [8–10]. In this group of conducting polymers, PANI has attracted considerable attention because of easy preparation, high yields from polymerization, and good environmental stability. Its surface charge characteristics can be easily modified by changing the dopant species in the material during synthesis. These composites of PANI have been synthesized with improved sensor properties [11, 12] and a list of potential materials, along with their limitations, used to develop the humidity sensor is given in Table 1.

Because the metal oxide, SnO_2, is a material with variable oxidation states and wide band gap (3.7 eV at 300 K) it proves as a useful material in chemical sensing [16], rechargeable batteries [17] and optoelectronic devices [18]. On the other hand, the limitation of a SnO_2 based sensor shows high

Electronic supplementary material The online version of this article (doi:10.1007/s00604-015-1678-2) contains supplementary material, which is available to authorized users.

✉ Saroj K. Shukla
sarojshukla2003@yahoo.co.in

✉ Sudheesh K. Shukla
sudheeshlshukla@gmail.com; sudheeshs@uj.ac.za

[1] Department of Polymer Science, Bhaskaracharya College of Applied Sciences, University of Delhi, New Delhi 190075, India

[2] Department of Applied Chemistry, University of Johannesburg, P.O. Box 17011, Doornfontein 2028 Johannesburg, South Africa

Table 1 Comparative study of the characteristics humidity sensor

Material	Sensing range (%)	Analytes and sensing methods	Response and Recovery time (s)	Limitations	References
PANI	3–80	Humidity and Electrical	30,80	Slow recovery	[13]
Chitin/ PANI	20–100	Humidity and Electrical	30, 180	Low range	[8]
SnO_2 (nano-wire)	30–85	Humidity and Electrical	120–170, 20–60	Low range	[14]
TiO_2/PPY	30–90	Humidity and Electrical	40	Low range	[10]
PANI /Mn_3O_4	20–50	Humidity and Electrical	–	Wide range	[15]
SnO_2/ PANI	5–95	Humidity and Electrical	26, 30	nil	Present work

operating temperature and a response variation due to structural changes at high temperature. In regards to conquer this drawback, doping of ions and its composites are reported [19, 20]. Furthermore, as PANI is a p-type organic semiconductor with a linear conjugate electronic system and SnO_2 is an n-type semiconductor, a composite of the two will have a p–n hetero-junction formation and it is proposed to have a better sensing platform than the pure individual constituents [21].

The humidity sensing mechanism on the SnO_2 is explained by the sorption of water molecules onto the surface, which alters the electronic conduction by depleting the charge carriers and inhibiting the charge-transduction process with the analyte [22]. Adsorption is usually described by the condensation of water molecules onto the sensor surface, which induces proton conduction and as a result causes a change in the net conductivity of the sensor. Different types of water layer structures (free water, liquid like and then ice like structure) develops on the humidity sensitive surface at different humidity ranges [23], regulating sensor efficiency.

Although there are variousthеories explaining the water sorption behavior on humidity sensing surfaces most of them contradict each other. It is important to understand the actual sensor mechanism in order to develop better humidity sensors [24]. The interfacial behavior and electronic band engineering between organic and inorganic materials are amongst the many explanations however the available literature reports have not provided conclusive evidence and therefore this particular angle will require further investigation [25]. In this paper we have introduced the sensitivity of the SnO_2/ PANI nanocomposite towards humidity. We claimed that the favorable electrical property of the nanocomposite was achieved through the synergistic effect of the individual components.

Experimental

Materials

$SnCl_2$ (99.95 %), $NaNO_3$ (99.5 %), KNO_3 (99.9 %), $CuSO_4$ (99.85 %), CH_3OH and aniline (99.5 %) were purchased from Sigma-Aldrich and used without further purification. All aqueous solutions were prepared with Mili-Q water and AR grade solvents were used.

Synthesis of SnO_2 and SnO_2/ PANI composites

5 mg of $SnCl_2$ was heated in $NaNO_3$-KNO_3 eutectic melt at 500 °C, where nano-size SnO_2 was formed [26]. 500 mg SnO_2 was dispersed in a mixture of aniline (2 mL) and methanol (5 mL). The resulting mixture was stirred for 30 min at room temperature on a magnetic stirrer and finally a transparent solution was obtained. After that, 5 mL aniline and 25 mL methanol was added with a 30 min stirring time over a magnetic stirrer at 25 °C. A 0.5 M aqueous cupric sulphate solution was then added drop-by-drop with constant stirring at room (~25 °C) temperature. Finally, a dark blackish-green precipitate was obtained. The precipitate was filtered using a wattman no. 1 filter paper and dried in a vacuum oven at 60 °C.

Characterization

The spectroscopy analysis was carried out using a Bruker (alpha) infrared spectrometer and 2501 PC (Shimadzu Corporation Japan) UV spectrometer. FTIR spectra were recorded in the KBr phase with an accumulation of 16 scan and a resolution of 4 cm^{-1} in the range of 4000 to 400 cm^{-1}. The particle phase, size and structure of the synthesized materials were studied using X-ray powder diffraction pattern on the Rigaku Rotaflex, RAD/Max-200B model X-ray diffractometer with CuKα (λ=1.5405 Å) radiation at a scanning rate of 2° per min. The surface morphology of the synthesized materials was examined by TEM, JEM-2100 model operated with a working voltage of 120 kV. In addition, isothermal thermogravimetric (TG) analysis was performed by measuring the mass of PANI and SnO_2/PANI pellet (diameter 13 mm and thickness 0.5 mm) using Shimadzu electronic balance with a minimum count of 0.1 mg. The mass measurement was carried out after exposure of the pellet at various relative humidity for 5 min. Thereafter, the pellet was successively heated at dehumidifying temperature (till a constant weight was obtained). The dehumidified pellet was kept in vacuum desiccators at room temperature (25 °C) for 24 h and

the weight was measured. The percentage water adsorption was calculated from Eq. 1 provided below,

$$\text{Water Contents} = \frac{Wx - Wo}{Wo} \times 100 \quad (1)$$

Where, W_x and W_o are the mass of the pellet at given relative humidity (RH) and in dry atmosphere, respectively.

Humidity sensing

In order to evaluate the humidity sensing behavior, a pellet of 13 mm diameter and 0.5 mm thickness was made by a hydraulic press after applying 8 t pressure for 10 min. The electrical contacts on the pellet were made by applying a layer of silver paste at the peripheral end. The probes of the multimeter were attached to the pellet at the contact points, while the other ends were connected to the Rish MAX multimeter. The schematic diagram of the experimental setup and details are reported in our earlier work [9]. In brief, the chamber was initially evacuated and subsequently a fixed relative humidity (RH) was maintained by putting a saturated salt solution [4]. The DC resistance of the pellet was measured as a function of RH maintained inside the chamber. Once the experiment was completed, the pellet was removed from the chamber and exposed to dry air to check the reversibility of the pellet.

Results and discussion

Material selection

Chen et al. [2] classified humidity sensing materials into three categories, namely; ceramic, semiconductor and organic polymer types. The ceramic materials like ZnO, MgO, NiO, Co_2O_3, Sb_3O_3, and SnO_2 are widely used for humidity sensing due to their adsorption capacity, porous structure and high temperature stability. Tin oxide adsorbs water molecules on the oxide surface in molecular and hydroxyl forms [26]. The water molecule behaves like a donor on the SnO_2 surface and dissociative adsorption generates hydroxyl and hydronium ions, which changes the electrical conductivity at lower temperature [27]. Therefore, SnO_2 humidity sensors based on semiconducting properties are expected due to fast competitive adsorption between H_2O and adsorbed oxygen species (O_2−, O−, etc.) and desorption of the adsorbed oxygen species and releasing of free electrons. This phenomenon suggests the electronic conduction mechanism and contribution of competitive adsorption between H_2O and adsorbed oxygen to changes the conductivity. However, as a typical metal oxide, SnO_2 has been used as a sensor material at a relatively high temperature (>200 °C) and limited RH range [28]. Thus, a humidity sensor based on SnO_2 will consume much energy when used for online detection. Therefore, it is necessary to develop new materials that work at room temperature, from the viewpoint of environmental protection and energy conservation [29]. The improvement in sensing properties is reported as the making of composites with polymers as well as a non-polymer matrix. In our earlier work we reported the ZnO/PANI nanocomposites as having an increased sensitivity. In this work we proposed the synergism between PANI and SnO_2 is because of their coordinating behavior, since PANI is a lewis base and SnO_2 is a lewis acid. The combination of both materials forms an efficient humidity sensing substrate.

Preparation of composite

The UV spectra of aniline and the SnO_2 dispersed in aniline solution are given in Fig. S1. Both spectra indicate a similar pattern with reduced absorbance in the SnO_2 dispersed in aniline solution. This reveals that when SnO_2 is mixed with aniline the aniline (weak lewis base) makes a layer around SnO_2 (weak lewis acid), thus lowering absorbance because of some intermolecular reaction between them. The physical parameters measured during polymerisation of pure aniline and SnO_2 modified with aniline are given in Table S1.

The temperature of the reaction bath containing the SnO_2-aniline mixture during polymerisation decreases by 7 °C, when compared to the bath of pure aniline. Since, polymerisation is an exothermic process; a decrease in temperature reduces the rate of de-polymerisation thus supporting polymerization of aniline. It may because of electron accepting nature (SnO_2) and electron donating nature (aniline). This route of synthesis makes the unstable aggregate of of metals over the polymerizing chain matrix under maintained temperature environment in reaction chamber. Therefore, further addition of the polymerizing agent, rapidly initiating the polymerization process where polymeric chains of aniline are formed, where one end attached to SnO_2. The synthetic route diagrammatized in scheme 1.

IR spectra

The FTIR spectra of PANI and SnO_2/PANI composite are given in Fig. 1. FTIR spectrum of PANI (Fig. 2b) shows the characteristic peaks i.e., (i) 586.65 cm^{-1} (C–N–C bonding mode of aromatic ring), (ii) 614 cm^{-1} and 691 cm^{-1} (C–C, C–H bonding mode of aromatic ring), (iii) 851.98 cm^{-1} (C–H out of plane bonding in benzenoid ring), (iv) 1050 cm^{-1} and 1167 cm^{-1} (aromatic ring deformation and benzenoid ring deformation, respectively), (v) 1495 cm^{-1} (C–N stretching of benzenoid ring) and (vi) 1606 cm^{-1} (C = N stretching of quinoid ring) [12]. While Fig. 1a showed the typical adsorption FTIR spectrum of SnO_2/PANI nanocomposites. A comparison study of PANI (Fig. 1b) and SnO_2/PANI composite (Fig. 1a), its reveals out that typical absorption peak of PANI

Scheme 1 Schematic illustration of sensing response of SnO_2/ PANI nanocomposite based humid sensor fabrication

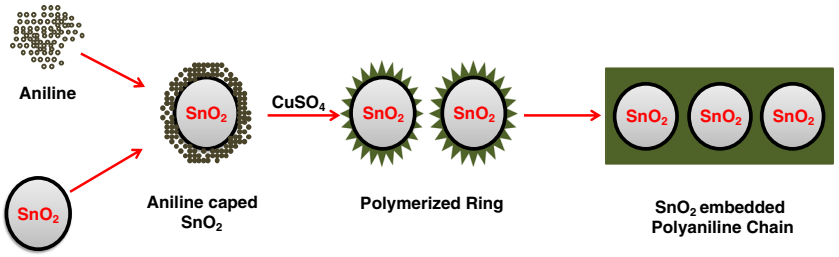

were spitted out with a remarkable wavenumber shifting. In Fig. 1a, the presence of characteristic peaks at 1113, 1022 and 956 cm-^{1} describes the presence of quinoid groups, while the peak at 901 and 752 cm^{-1} is attributed to C-H stretching planes. Hence, FTIR spectra confirm the formation of heterogeneity in the polymeric chain matrix due to the presence of SnO_2. Whereas, the FTIR absorption peak at 423, 603 and 717 cm^{-1} is due to the presence of metal oxide i.e., SnO_2 [30].

XRD

X-ray diffraction pattern of the prepared SnO_2, PANI and SnO_2/PANI composite are shown in Fig. 2. The diffraction pattern of SnO_2 shows broad and well-defined peaks, which indicates the crystalline nature of the synthesized materials. The observed 2θ values for the pure SnO_2 diffraction pattern, matches well with the standard values (JCPDS# 41–1445), and hence confirms the tetragonal phase of SnO_2. Furthermore, the average crystallite size of SnO_2 was calculated by (110), (101) peaks, employing the Debye-Scherrer formula [5, 31]. The calculated mean size of synthesized SnO_2 nanoparticles was found to be of 45 nm.

The XRD pattern of the SnO_2/PANI composite shows an identical diffraction pattern to that of polyaniline and tin oxide. This information indicates that the SnO_2/PANI composite has an identical profile as the pure SnO_2 particle and PANI. However the intensity of the composite peaks is observed to be lower than pure PANI and SnO_2. This reduction in peak intensity indicates the decrease in crystallinity of the composite material; implying that the insertion of SnO_2 nano particles hindered the crystallization of polyaniline chains in the hybrid nanocomposites during their formation [32].

Morphological study and elemental analysis

Figure 3a and b show the TEM image and EDX spectrum of SnO_2 nanoparticles, respectively while Fig. 3c shows the TEM image of the SnO_2/PANI nanocomposite. The Fig. 3a reveals nano sized particles of tin oxide with spherical shape and regular morphology, while EDX spectrum indicates the presence of tin and oxygen peak as main constituents and corroborates the synthesis of SnO_2 nanoparticles. The micrograph of the composite reveals a binary structure because of the presence of SnO_2 and PANI. In addition the micrograph of the composites illustrates the presence of pores. These pores are responsible for improving the adsorption properties of the composite as well as enhancing the sensing response for the fabricated sensors.

UV spectra

The UV–Vis spectrum (Fig. S2) shows the characteristic peaks of PANI and SnO_2/PANI composite. In the PANI spectra the absorbance peaks found at 324, 483 and 583 nm are

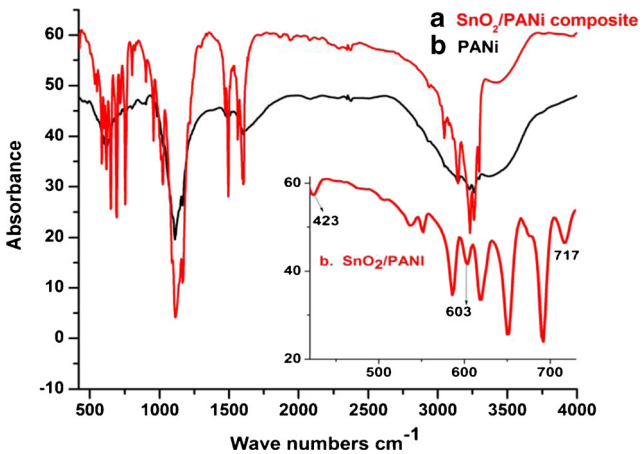

Fig. 1 FT-IR spectra in KBr monitored in the region between 4000 cm^{-1} and 500 cm^{-1} of **a** SnO_2/ PANI composite and **b** PANI

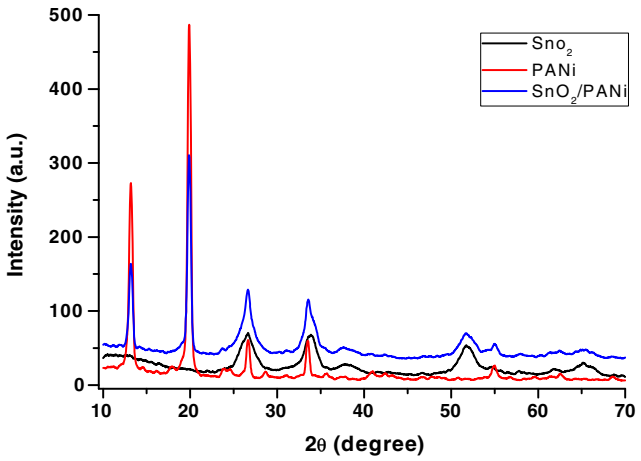

Fig. 2 X-Ray diffraction pattern of SnO_2, PANI and SnO_2/ PANI composite

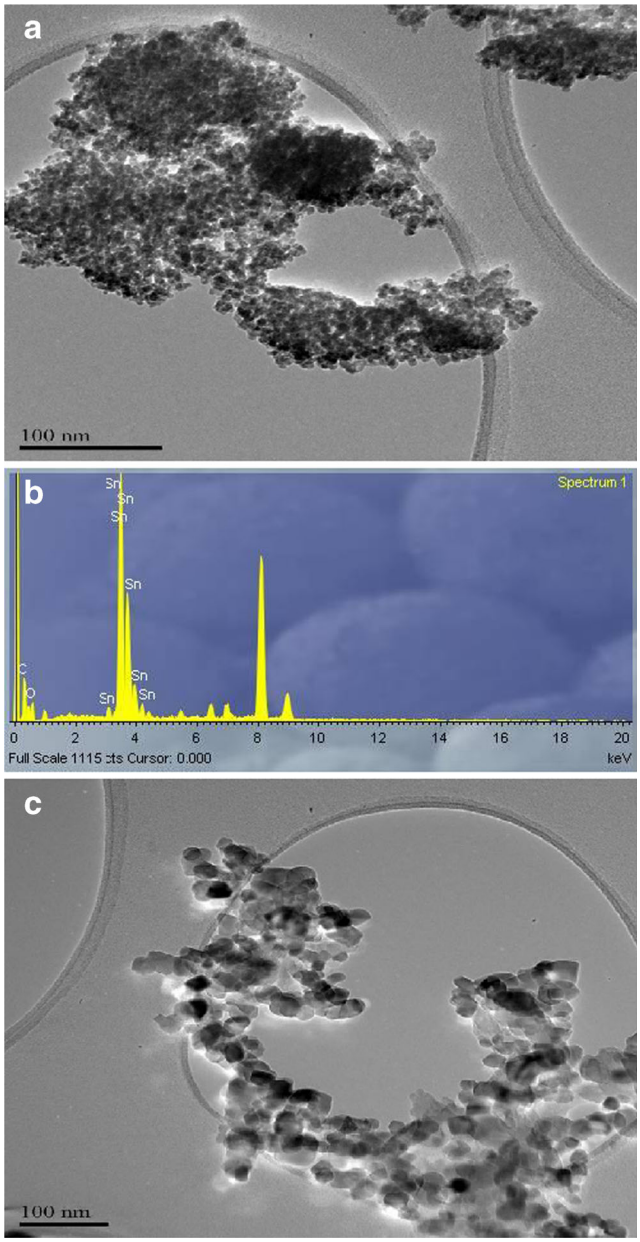

Fig. 3 Transmission electron micrograph of **a** SnO_2 nanoparticle and **c** of SnO_2/ PANI nanocomposites; while **b** EDX spectrum of SnO_2 nanoparticle

due to π-π*, π–polaron and π–bipolaron transitions, respectively [6]. Although the shape of UV spectra of nanocomposites is similar to PANI, a remarkable shifting of bands is noticed at 312, 465 and 572 nm. In the composite, the peaks between 400 and 600 nm is ascribed to the selective interaction between SnO_2 and the quinoid ring of PANI. The addition of SnO_2 promotes the increase in band intensity which is primarily due to interactions between SnO_2 and PANI molecules while the wavelength decreases due to the interaction between oxygen in SnO_2 (due to acidic nature) and -NH (basic nature) in PANI [30]. The characteristic peak of SnO_2 cannot be detected which is supposedly due to a low amount of SnO_2 in the composite materials.

Humidity sensing behavior

The trend for the change in electrical resistance with different relative humidity (RH) values is provided in Fig. 4. The curve reveals a continuous decrease in resistance of composites with an increase in humidity range from 5 to 90 % RH. This effect may be attributed to the dissociative adsorption of H_2O on the nano-composite surface [9, 31]. The change in resistance of PANI with RH values is also given in the inset of Fig. 4. The curve reveals the lesser linear change in pure PANI up to 60 % RH while in the nano composite linear change is up to 70 % RH. Again, it is proposed that a synergism exists between the hydrophilicity of SnO_2 and hydrophobicity of PANI. A similar result is reported by Zhuo et al., where doping of antimony (Sb) in SnO_2 was carried out in order to improve the humidity sensitivity between the ranges of 20 to 40 RH. The sensitivity of the sensor element towards humidity was calculated as per the reported method [32] and was found to be 0.22 % RH while in pure PANI was recorded at 0.025, which is ten times lower than the prepared SnO_2/PANI nano composite.

The sensor response of the composite at different humidity was calculated by using Eq. 2 for both PANI and for the SnO_2/ PANI composite.

$$S(\%) = \frac{R - R_0}{R_0} \times 100 \tag{2}$$

In Eq. 2, R_o and R are the initial and final resistance of the pellet at particular humidity, respectively. Figure 5 shows the sensing response curve of SnO_2/PANI nanocomposite in respect to different RH value. The result reveals the linear sensing range in PANI is at 60 % RH but SnO_2/PANI nanocomposite improves up to 70 % RH. The significant improvement

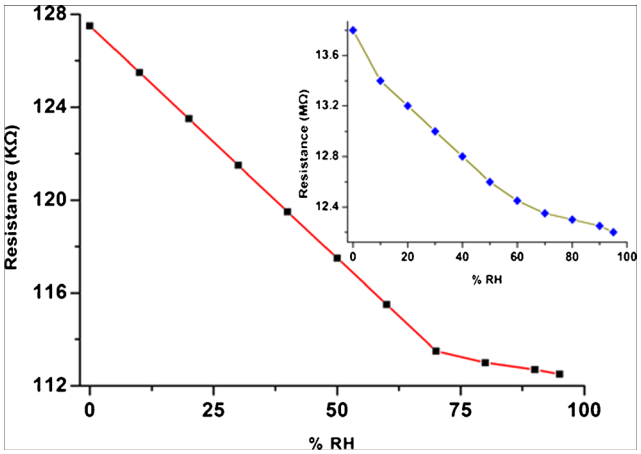

Fig. 4 Change in resistance with relative humidity of SnO_2/PANI and PANI in inset

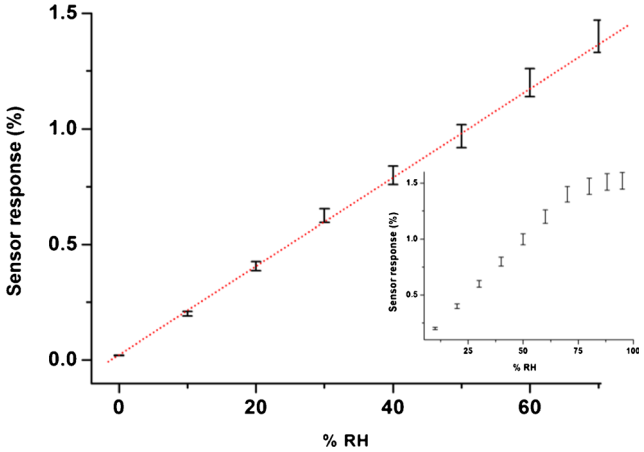

Fig. 5 Sensing response curve of SnO_2/PANI nanocomposite at different relative humidity

in the sensing behavior may be due to the tuning of the surface energy of SnO_2 and the polyaniline composite.

A further change in resistance is measured against time at 70 % RH shown in Fig. 6. The graph indicates a 90 % increase in resistance in 26 s at 70 % RH value and again returns to the original value in 30s after dehumidifying the chamber. This result infers that the response time (time required to reach 90 % of the final equilibrium value) of the sensor is 26 s while the recovery time was 30s [9]. The lifetime of the SnO_2/PANI based sensor was determined by measuring the resistance up to 6 months at an interval of 7 days. It was found that the sensitivity was constant up to a 6 month period but after 6 months, the sensitivity decreased at a very slow to about 7 %. The interference behavior of the sensor was studied against acetone, ethanol and ammonia by adding 5 %*v/v* mixture in the chamber. The results are given in Table S2. During the interference study, it was found that interferents had a negligible effect (3 %) at %RH ranging from 5 to 70.

The reproducibility of the sensor response for the probe was investigated at a 70 % RH with no significant decrease in sensitivity response observed even after 10 cycles. This data shows the good responsibility of the proposed humidity sensor. The relative standard deviation was found to be ±3 % determined by five successive measurements of a 70 % RH standard using a single probe. In a series of 10 sensors using 10 different sensing pellets probes, a relative standard deviation of about±3 % was obtained for the individual sensing response at constant 70 % RH. Table 1 compares the characteristics of different nano-sized based humidity sensors reported in the literature. It clearly reveals that most of the reported humidity sensors are not widely adaptable due to their limited operational range, cost effectiveness and hazardous nature. Thus, present nano SnO_2/PANI based probe exhibited as an efficient humidity sensor with wider operational range, higher selectivity and sensitivity at ambient conditions. This study indicates that the incorporation of SnO_2 in the polyaniline matrix enhances the hydrophilicity and therefore successively increases the sensing behavior. The improvement in sensing behavior can also be understood as polymers are known for their low surface energy, making them less suitable for sensing purposes [33]. But the incorporation of SnO_2 in polyaniline improves the surface for a better sensing platform due to an increase in surface energy for effective sensing purposes.

The inference study was also carried out for SnO_2/PANI nanocomposite based fabricated humidity sensor (Fig. 7) against polluting gases (SO_2 and NO_2) and also followed by acetone, ethanol and ammonia. The interferent's investigation showed that the effect of interference of polluting gases (SO_2 and NO_2) is more than the other respective interferents i.e., acetone, alcohol and NH_3, but the effect of effect of interference is below the 3 %. This may be due to the acidic nature of gases. Due to acidic nature of gases, there is higher possibility of doping the H^+ and thus resultant conductance increased.

In addition, humidity sensor also interfered by ozone (O_3), particularly in sunny countries [36]. The performance of SnO_2/PANI nanocomposite based fabricated humidity sensor

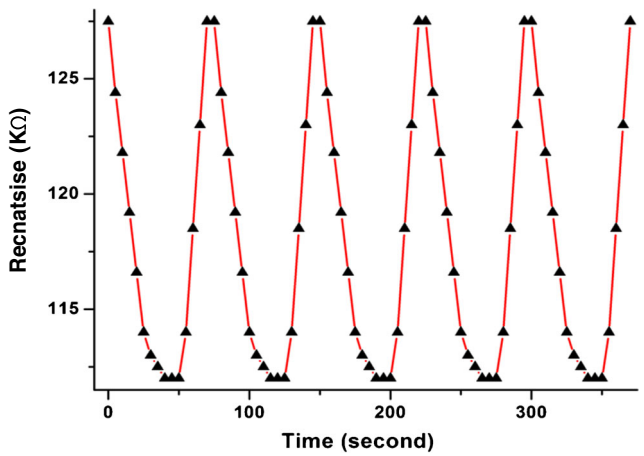

Fig. 6 Change in resistance with time at fixed humidity

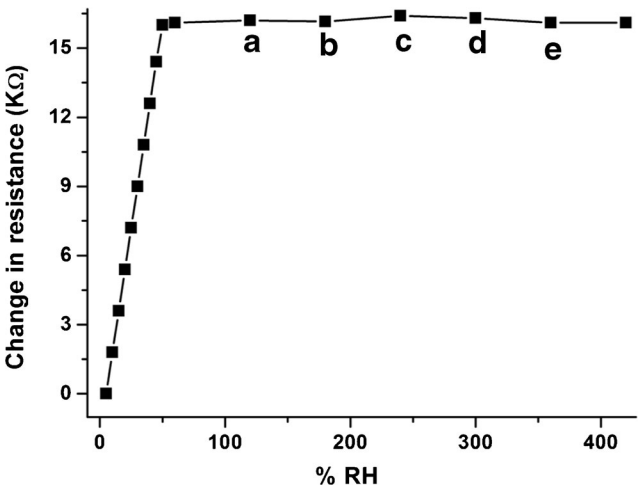

Fig. 7 **Figure**: Interference study of SnO_2/PANI nanocomposite based fabricated sensor against **a** acetone, **b** alcohol, **c** SO_2, **d** NO_2 and **e** NH_3

also interfered by O_3 but below the 3 %. In our ongoing lab work we are focusing our investigation in this affair.

Water growth kinetics and sensing model

Water adsorption on solid surfaces is ubiquitous in nature and highly interdisciplinary in nature. The interfacial adsorption is a topic of interest in catalysis, environmental science, atmospheric chemistry, electrochemistry, corrosion chemistry and sensing science. The adsorbed water molecules on surfaces influence the surface chemical reactions and develop the induced charges. The mass change due to moisture adsorption and dehydration temperature of the prepared SnO_2/PANI composite at different RH value is shown in Table S3. The results predict that the extent of maximum adsorption increases with an increase in RH from 5 % to 70 %, while anything above this yields less adsorption. This observation indicates that the adsorption of water on a composite surface forms a monolayer to multilayer surface with an increase in water vapor pressure up to 70 % RH. But with subsequent increase in RH, the adsorption modes change from layer formation to capillary condensation and may form three dimensional networks due to pores present in materials. This emphasizes the significant role of the pore diameter, as calculated by (Eq. 3):

$$rk = \frac{2\gamma M}{\rho RT \ln P_s \Big/ p} \tag{3}$$

Where, rk is the radius, γ is surface tension, ρ is density and M is molecular mass of H_2O molecules. P_s is saturated vapor pressure and P is vapor pressure at fixed atmospheric condition.

Desorption temperature also shows comparable results up to 70 % RH, but above 70 % RH desorption temperature increases by 30 °C. This result validates that adsorption takes place at first layer and also followed by the capillary condensation, at higher relative humidity. Based on this data, it is likely that the percolation of the solid surface model does not apply up to 70 % RH, since percolated molecules require higher energy to dissociate and are also desorbs at 162 °C [34]. In this case, water desorbs at 152 °C, thus, it seems that the hydration proceeds occur through a diffusion suspension layer model. Where, H_2O molecules interact with the polymeric matrix and results in the formation of hydrate-like particles suspended on the surfaces. This aggregate type clusters is probably due to the reduction in hydrophilicity of SnO_2 because of the presence of hydrophobic aniline. This inadvertently becomes suitable for better humidity sensing [35]. After that, suspended molecules may diffuse into the nanocomposite matrix and percolation proceeds gradually in the matrix. This can be attributed to the spongy surface of the composite rather than a condensate in case of ceramic. The spongy surface bears greater permeability of water molecules, thus water vapor molecules can easily pass through the pore openings and serves as a better sensing platform. Novelty of this work is that we proposed 10 times sensitivity and 20 % improved linear sensing range than earlier reported. This study divulges the significance contribution and synergism between counterpart components of nanocomposites, in regards to improvement of sensitivity and linear sensing range. The other novelty of this work is to improvement in the polymerization on lowering the temperature by 7 °C than earlier reported and this makes process easier and cost effective.

Conclusions

Nano size SnO_2 and SnO_2/PANI nanocomposite was synthesised by a simple chemical route. The electrical resistance of the SnO_2/PANI nanocomposite continuously decreased from 127.5 KΩ to 114 KΩ with an increase in relative humidity from 5 to 95 % RH. The results validated that the prepared nanocomposite was suitable for humidity sensing with an improvement in the sensing range (increased sensitivity by 10 times), 20 % linearity, and response time. The isothermal TG data indicated that synergism between surface properties of composite materials can be an effective strategy to develop better sensing platforms with a tunable sensing range due to optimised surface energy and sensing model for individual gaseous molecules. The synthesized SnO_2/PANI nanocomposite was suitable for humidity sensing by an electrochemical method with better sensitivity, linearity, and quicker response time. The sensing mechanism with a hydrate formation model has been proposed to understand the sensing behavior of the material. The observed data indicates that synergism between surface properties of composite materials can be an effective strategy to develop better sensing platforms with a tunable sensing range due to optimised surface energy and sensing model for individual gaseous molecules.

Acknowledgments The authors wish to acknowledge the University Grant Commission (MRP. 8-3(47)/2011), New Delhi for generous financial support to carry out this work. SKS and ESA also acknowledge financial support from Global Excellence and Stature (GES) fellowship from the University of Johannesburg. Authors are thankful to the reviewers for their constructive comments to improve the quality of manuscript.

References

1. Fraden J (2010) Handbook of modern sensors physics, designs, and applications, 3rd edn. Springer, New York
2. Chen Z, Lu C (2005) Humidity sensors: a review of materials and mechanisms. Sens Lett 3:274–295
3. Fernandez-Garcıa M, Martınez-Arias A, Hansonand JC, Rodriguez JA (2004) Nanostructured oxides in chemistry: characterization and properties. Chem Rev 104:4063–4104

4. Shukla SK, Parashar GK, Mishra AP, Mishra P, Yadav BC, Shukla RK, Bali LM, Dubey GC (2004) Nano-like magnesium oxide films and its significance in optical fiber humidity Sensor. Sens Actuators B 98:5–11
5. Shukla SK, Tiwari A, Parashar GK, Mishra AP, Dubey GC (2009) Exploring fiber optic approach to sense humid environment over nano-crystalline zinc oxide film. Talanta 80:565–571
6. Shukla SK, Bharadvaja A, Tiwari A, Parashar GK, Mishra AP, Dubey GC (2012) Fabrication of ultra-sensitive optical fiber based humidity sensor using TiO_2 thin film. Adv Mater Lett 3:365–370
7. Yiheng QY, Howlader MR, Deen MJ, Haddara YM, Selvaganapathy PR (2014) Polymer integration for packaging of implantable sensors. Sens Actuators B 202:758–778
8. Ramprasad AT, Rao V (2010) Chitin-polyaniline blend as a humidity sensor. Sens Actuators B 148:117–125
9. Shukla SK (2013) Synthesis and characterization of polypyrrole grafted cellulose for humidity sensing. Int J Biol Macromol 62: 531–536
10. Su P-G, Huang L-N (2007) Humidity sensors based on TiO_2 nanopaticles/polypyrrole composite thin films. Sens Actuators B 123:501–507
11. Shukla SK, Vamakshi, Minakshi, Bharadavaja A, Shekhar A, Tiwari A (2012) Fabrication of electro-chemical humidity sensor based on zinc/polyaniline nanocomposites. Adv Mater Lett 3:421–425
12. Shukla SK (2012) Synthesis of polyaniline grafted cellulose suitable for humidity sensing. Ind J Eng Mater Sci 19:417–420
13. Shukla SK, Bharadvaja A, Tiwari A, Pilla S, Parashar GK, Dubey GC (2010) Synthesis and characterization of highly crystalline polyaniline film promising for humid sensor. Adv Mater Lett 1: 129–134
14. Quang Q, Lao C, Wang ZL, Xie Z, Zhang ZL (2007) High-sensitivity humidity sensor based on a single SnO_2 nanowire. J Am Chem Soc 129:6070–6071
15. Singla ML, Awasthi S, Srivastava A (2007) Humidity sensing: using polyaniline/Mn_3O_4 composite doped with organic/inorganic acid. Sens Actuators B 127:580–585
16. Ying Z, Wan Q, Song ZT, Feng SL (2004) SnO_2 nanowhiskers and their ethanol sensing characteristics. Nanotechnology 15:1682
17. Peng Z, Shi Z, Liu M (2000) Mesoporous Sn-TiO_2 nanocomposite electrodes for lithium batteries. Chem Commun 21:2125–2126
18. Aoki A, Sasakura H (1970) Tin oxide thin film transistors. J Appl Phys 9:582–584
19. Ma N, Suematsu K, Yuasa M, Kida T, Shimanoe K (2015) Effect of water vapor on Pd-loaded SnO_2 nanoparticles gas sensor. ACS Appl Mater Interfaces 7:5863–5869
20. Bing Y, Zeng Y, Liu C, Qiao L, Sui Y, Zou B, Zheng W, Zou G (2014) Assembly of hierarchical $ZnSnO_3$ hollow microspheres from ultra-thin nanorods and the enhanced ethanol-sensing performances. Sens Actuators B 190:370–377
21. Murugan C, Subramanian E, Pathinettam DP (2014) Enhanced sensor functionality of *in situ* synthesized polyaniline–SnO_2 hybrids toward benzene and toluene vapors. Sens Actuators B 205: 74–81
22. Parvatikar N, Jain S, Khasim S, Revansiddapp M, Bhoraskar SV, Prasad A (2006) Electrical and humidity sensing properties of polyaniline/WO_3 composite. Sens Actuators B 114:599–603
23. Assay DB, Kim SH (2005) Evolution of the adsorbed water layer structure on silicon oxide at room temperature. J Phys Chem B 109: 16760–16763
24. Li Q, Li Y, Yang M (2012) Investigation on the sensing mechanism of humidity sensor based on electrospun polymer nanofibers. Sens Actuators B 171–172:309–314
25. Barsan N, Schweizer-Berberich M, Göpel W (1999) Fundamental and practical aspects in the design of nanoscaled SnO_2 gas sensor: a status report. Fresenius J Anal Chem 365:287–304
26. Rastogi RP, Shukla SK, Singh NB (2010) Synthesis of NiO nano crystal though nitrate eutectic melt. Ind J Eng Mater Sci 17:477–480
27. Korotchenkov G, Brynzari V, Dmitriev S (1999) Electrical behavior of SnO_2 thin films in humid atmosphere. Sens Actuators B 54:197–201
28. Batzill M (2006) Surface science studies of gas sensing materials: SnO_2. Sensors 6:1345–1366
29. Popova LI, Andreev SK, Gueorguiev VK, Stoyanov ND (1996) Pulse mode of operation of diode humidity sensors. Sens Actuators B 37:1–5
30. Mostafaei A, Zolriasatein A (2012) Synthesis and characterization of conducting polyaniline nanocomposites containing ZnO nanorods. Prog Nat Sci Mater Int 22:273–280
31. Shukla SK, Singh NB, Rastogi RP (2015) Nanosize SnO_2 through nitrate eutectic mixture for humidity sensors. Emerg Mater Res 4(1):27–43
32. Zhuo M, Chen Y, Sun J, Zhang H, Guo D, Zhang H, Li Q, Wang T, Wan Q (2013) Humidity sensing properties of a single Sb doped SnO_2 nanowire field effect transistor. Sens Actuators B 186:78–83
33. Agastino R, Favia P, Oehr C, Wertheimer MR (2005) Low-temperature plasma processing of materials: past, present and future. Plasma Process Polym 2:7–15
34. Gercher VA, Cox DF (1995) Water adsorption on stoichiometric and defective SnO_2(110) surfaces. Surf Sci 322:177–184
35. Matsuguchi M, Umeda S, Sadaoka Y, Sakai Y (1998) Characterization of polymers for a capacitive-type humidity sensor based on water sorption behavior. Sens Actuators B 49:179–185
36. Ando M, Swart C, Pringsheim E, Mirsky VM, Wolfbeis OS (2005) Optical ozone-sensing properties of poly(2-chloroaniline), poly(*N*-methylaniline) and polyaniline films. Sems Actuators B 108:528–534